Biointerface Research in Applied Chemistry
Platinum Open Access Journal (ISSN: 2069-5837)

Article
Volume 12, Issue 1, 2022, 170 - 179
https://doi.org/10.33263/BRIAC121.170179

Influence of Fe_2O_3 Dopant on Dielectric, Optical Conductivity and Nonlinear Optical Properties of Doped ZnO-Polystyrene Composites Films

Samia Ahmed Gad [1], Hala Abomostafa [2], Mohamed M. Selim [3], Ahmed Abdel Moez [4,*]

1 Solid State Electronics Laboratory, Solid State Physics Department, Physical Research Division, National Research Centre, 33 El-Bohouth Street, Dokki, Giza 12622, Egypt; samiagad2000@yahoo.com (S.A.G.);
2 Faculty of Science, Physics Department, Menoufia University, Egypt; halaabomostafa@yahoo.com (H.A.);
3 Physical Chemistry Department, National Research Centre, El-Bohouth Street, 12622, Dokki, Giza, Egypt; mmaselim@yahoo.com (M.M.S.);
4 Semiconductor Laboratory, Solid State Physics Department, Physical Research Division, National Research Centre, 33 El- Bohouth Street, Dokki, Giza 12622, Egypt; aam692003yahoo.com (A.A.M.);
* Correspondence: aam692003yahoo.com (A.A.M.);

Scopus Author ID 57034126200
Received: 23.02.2021; Revised: 1.04.2021; Accepted: 5.04.2021; Published: 19.04.2021

Abstract: ZnO-Polystyrene nanoparticles doped with Fe_2O_3 were prepared by the casting method. Both E_d and E_o were calculated. ε_L and N/m^* increase with filler concentrations for these samples. On the other hand, both M_{-1}, M_{-3}, decreased with increasing filler. The filler concentrations affected on determined values of both of $\varepsilon^{\backslash}$ and $\varepsilon^{\backslash\backslash}$. These values increase with filler, and also the same result was achieved for both σ_1 and σ_2, which also increases with filler. The relation between VELF and SELF was determined. $\chi^{(1)}$ increases with increasing filler ratio. n_2, $\chi_{(3)}$, β_c, were determined theoretically. The electrical susceptibility χ_e and relative permittivity ε_r increase with the increase of filler concentration as a result of increasing electron mobility.

Keywords: Fe_2O_3 doped with ZnO-polystyrene nanoparticles; dielectric properties; optical conductivity; nonlinear optical properties.

1. Introduction

have a great interest due to their properties and wide electronic applications [1–4]. Polymer composites are widely used as electrically conductive glues. Polystyrene has high transparency and is used for industrial applications [5, 6] such as chromatography [7], sorption processes [8], sensors [9, 10], biomedical applications [11–12], and other electronic applications [13–14]. Polymers' matrix properties can be improved by the dispersion of metals in the polymer matrix [15, 16]. Zinc Oxide is a magic material as a result of its properties [17–19]. It has a direct bandgap (E_g = 3.25 eV) [20], which is a promising material for optoelectronic applications [21, 22]. On the other hand, ZnO material had some disadvantages, such as a low quantum efficiency [23], so reinforcing particles must be added to ZnO matrix composite, such as Fe_2O_3 because of its thermodynamic stability, high resistance to photo-corrosion, and narrow bandgap of 2.2 eV. So, Fe_2O_3 is an important member of visible-light-responsive semiconductor photocatalysts [24–27]. Different methods have been used to synthesize various metal-polymer composites, such as the sol-gel process [28], mixing route of polymer with metal solution [29], chemical oxidation [30], and in-situ techniques [31]. The optical properties of ZnO-Polystyrene

had been studied [32–36]. It was found that the transmitted spectra are increased with ZnO ratio [32], ZnO percentage had increased absorption ratio for polystyrene [34], ZnO-PS nanocomposite is highly transparent throughout the visible region [35], the energy gap decreased with ZnO ratios for ZnO/PS composite [36]. The doping effect on the optical properties of ZnO/ Polystyrene films had been studied [37]. The direct energy gap decreased with increasing Fe_2O_3 for ZnO Polystyrene. The nonlinear optical properties of ZnO-Polystyrene composites had been investigated [38–39]. It was noticed that PS had good applications for nonlinear optical devices [39]. In this work, we investigated the effect of Fe_2O_3dopant on nonlinear optical properties such as (nonlinear refractive index, nonlinear absorption coefficient, third-order nonlinear optical susceptibility, and semiconducting results for ZnO/Polystyrene composites films.

2. Materials and Methods

Fe_2O_3 doped ZnO powder was prepared by auto combustion method through mixing zinc nitrate, iron nitrate, and urea as an oxidizing agent with a certain calculated ratio. The mixed powders were placed in porcelain crucible to be burned in the furnace at about 370°C until the mixture homogenates, self-sustaining and rather fast combustion with enormous swelling producing white foamy and voluminous Fe_2O_3doped ZnO. Then, furnace's temperature was increased up to 500°C, and the mixture was heated at this temperature for two hours before the furnace is switched off. Polystyrene (PS) was used as received without further purification with (MW= 35000 softening point (ASTM 28) 123-128 °C, density 1.06 g/mL at 25 °C from Sigma-Aldrich ,Germany). The appropriate weight (5gm) of PS was dissolved in 100 ml of chloroform. The mixture was magnetically stirred continuously at room temperature for 2 hours until the mixture solution has a homogenous viscous appearance. The solution was left for 3 days before the addition of metal oxides filler to it. Different weights of the prepared powder with (5, 7.5, 10, and 12.5 wt. %) were added to the chloroform and magnetically stirred vigorously to ensure a high dispersion of the added nanoparticles for 1 hour and then ultra-sonication for another 1 hour to prevent the agglomeration of the nanoparticles. The mixture was then mixed with the PS solution and stirred again for 1 hour, then ultra-sonication for 1 h. The polymers PS's final product reinforced with Fe_2O_3 doped ZnO nanoparticles was cast in glass Petri dishes and left 1 day for drying. The optical measurements of the prepared films were investigated using UV- Vis spectrophotometer type JASCO 570.

3. Results and Discussion

3.1. Dielectric, optical conductivity, and linear optical susceptibility results.

The films based on polystyrene (PS) filled with different concentrations of ZnO doped with Fe_2O_3 had a polycrystalline structure [37]. The oscillator energy E_o and is the dispersion energy E_d were expressed as [40]:

$$n^2(E)-1=\frac{E_o \cdot E_d}{E_o^2-E^2}$$

$$n^2 - k^2 = \varepsilon_L - \left(\frac{eN}{4\pi c^2 \varepsilon_o m^*}\right)\lambda^2$$

E is the photon energy. The dependence of $(n^2\text{-}1)^{-1}$ on (photon energy)^2 $(h\nu)^2$ is shown in figure 1(a). The behavior of $(n^2\text{-}1)^{-1}$ is the same for all studied samples. The values for both E_o and E_d decreased with increasing the filler concentration. This is due to decreasing the E_{gdir} for these samples with filler [37], which allows electrons to absorb energy with lower values, and the vibration of these electrons decreases. Figure 1(b) shows the relation between n^2 and λ^2, N/m* values were determined using [41]:

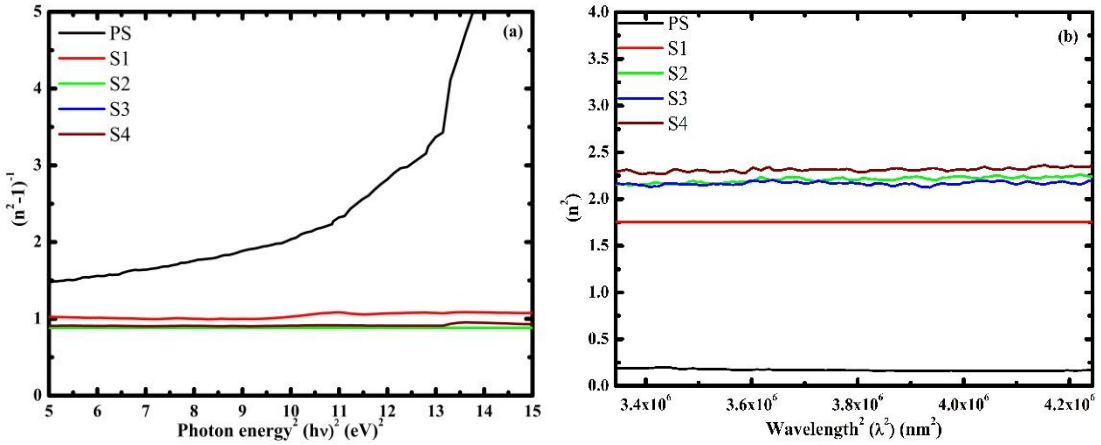

Figure 1. (**a**) The relation of $(n^2\text{-}1)^{-1}$ and $(h\nu)^2$; (**b**) the relation of n^2 and λ^2 for ZnO films doped with Fe_2O_3.

The value of N/m* increases with filler concentrations because of the increased free electrons with filler. The M_{-1} and M_{-3} derived from the relations [41]:

$$E_o^2 = \frac{M_{-1}}{M_{-3}}$$

$$E_d^2 = \frac{M_{-1}^3}{M_{-3}}$$

Table 1 shows the values of M_{-1} and M_{-3} for these thin films.

Table 1. Results table for ZnO-polystyrene composites films doped with Fe_2O_3.

Sample	ε_L	E_o (eV)	E_d (eV)	M_{-1} (eV)	M_{-3} (eV)	(f) $(eV)^2$	n_o	N/m*
PS	0.20	6.10	8.30	6.91	2.85	47.79	1.55	9.1E+50
S1	0.28	5.90	8.10	5.99	2.51	35.91	1.54	1.5E+51
S2	2.10	5.70	6.30	5.35	2.28	28.60	1.45	3.1E+51
S3	2.25	5.50	5.20	4.59	2.21	21.07	1.39	4.9E+51
S4	2.30	4.30	4.90	4.59	2.21	21.07	1.46	6.2E+51

The oscillator strength *f* was calculated as following [42]:

$$f = E_o \cdot E_d$$

The values of *f* decrease with filler, as a result of decreasing both of E_o and E_d. Another important parameter depending on E_o and E_d is that static refractive index n_o, which was determined as [43]:

$$n_o = \left[\left(E_d / E_o\right) + 1\right]^{0.5}$$

The dielectric loss ε\ and dielectric tangent loss ε\\ for these films were calculated as follows [44]:

$$\varepsilon^{\backslash} = (n^2 + k^2)$$

$$\varepsilon^{\backslash\backslash} = \left[(n^2 + k^2)^2 - (n^2 - k^2)^{0.5}\right]$$

The effect of hν on both of ε\ and ε\\ is shown in Figures 2(a,b), from this figures both of ε\ and ε\\ had the same behavior with hν for all these samples, while ε\ and ε\\ increase with filler concentration, due to increasing the packing density[37].

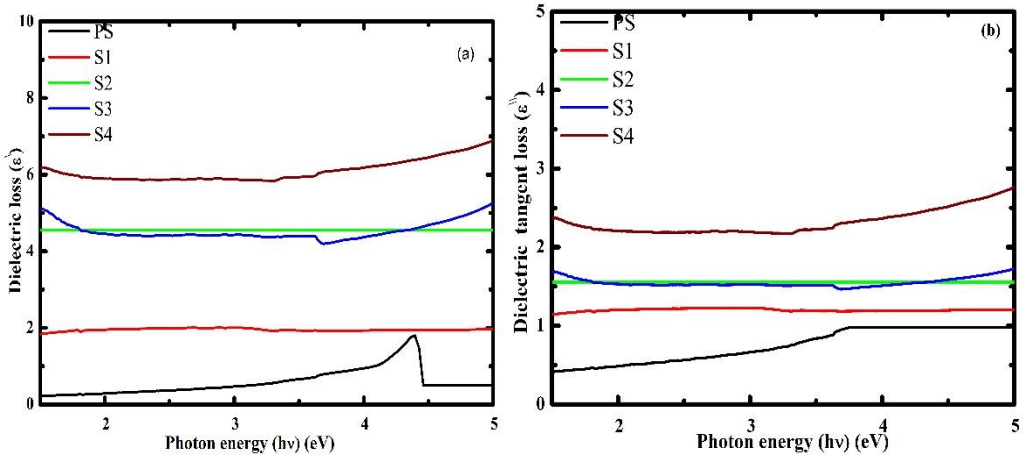

Figure 2. Dependence of (**a**) ε\; (**b**) ε\\ on hν for ZnO films doped with Fe_2O_3.

The optical conductivity was calculated from the following equations [45]:

$$\sigma_1 = \left(\frac{\varepsilon^{\backslash\backslash} \cdot c}{2\lambda}\right)$$

$$\sigma_2 = \frac{(1 - \varepsilon^{\backslash}) \cdot c}{4\lambda}$$

Figures 3(a,b) show σ_1 and σ_2 dependence on hν for these films, σ_1 and σ_2 increase with filler ratios and hν for these samples, this due to increasing the electron mobility's with filler.

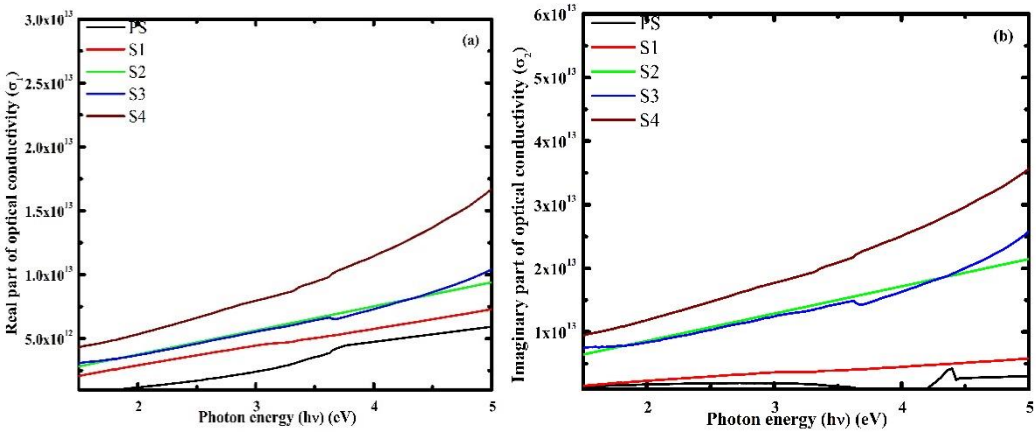

Figure 3. Influence of hν on (**a**) σ_1; (**b**) σ_2 for ZnO films doped with Fe_2O_3.

Both of (VELF) and (SELF) for these samples were determined using [41]:

$$VELF = \frac{\varepsilon''}{\varepsilon'^2 + \varepsilon''^2}$$

$$SELF = \frac{\varepsilon''}{(\varepsilon' + 1)^2 + \varepsilon''^2}$$

The relation between VELF/SELF for these thin films is shown in Figure 4(a). Linear optical susceptibility $\chi^{(1)}$ describes the response of the material to an optical wavelength, $\chi^{(1)}$ was determined as[46]:

$$\chi^{(1)} = \frac{(n^2 - 1)}{4\pi}$$

The relation between $\chi^{(1)}$ and hν for these films is shown in Figure 4(b). $\chi^{(1)}$ increased with increasing filler ratio. This means that there is a possibility for changing optical properties with slight doping for these samples.

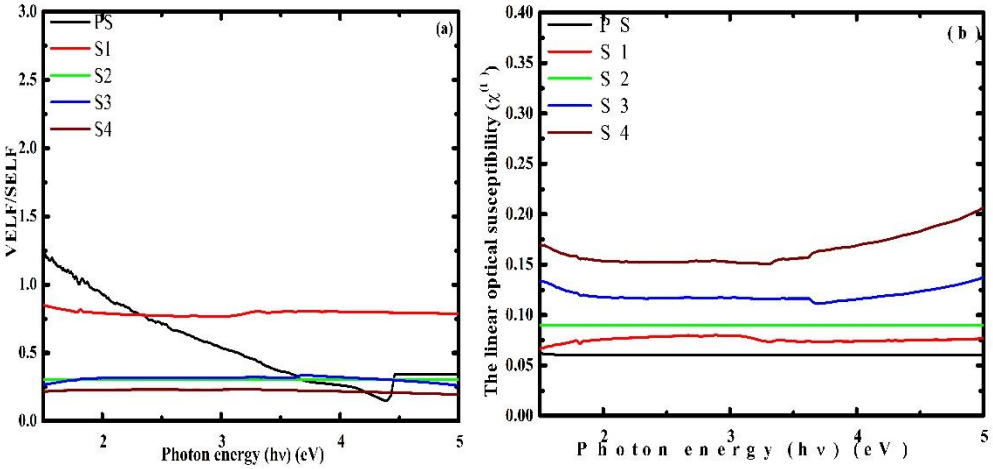

Figure 4. (**a**) Relation between (VELF/SELF) and (hν); (**b**) relation between $\chi^{(1)}$ and hν for ZnO films doped with Fe_2O_3.

3.2. Nonlinear optical properties.

The nonlinear refractive index n_2 was determined as [48–49]:

$$n_2 = \left(12\pi\chi^{(3)}\right) / n_o$$

The dependence of n_2 on λ is in figure 5(a). n_2 increase with filler due to an increase in the packing density [37]. An important parameter is the third-order nonlinear optical susceptibility $\chi^{(3)}$, which was determined as [50]:

$$\chi^{(3)} = A\left[\frac{E_o \cdot E_d}{4\pi(E_o^2 - (h\nu)^2)}\right]^4$$

where, A =1.7 x 10^{-10} e.s.u [50]. $\chi^{(3)}$ dependence on and hν is shown in figure 5(b). $\chi^{(3)}$ increases with hν and also with filler concentrations. On the other hand, nonlinear absorption coefficient β_c was determined as follows [51]:

$$\beta_c = \frac{48 \cdot \pi^3 \chi^{(3)}}{n^2 c \cdot \lambda}$$

Figure 5(c) shows the influence of hν on β_c, β_c increase with filler because of high values of filler concentrations, the access number of electrons, and a large number of excited electrons.

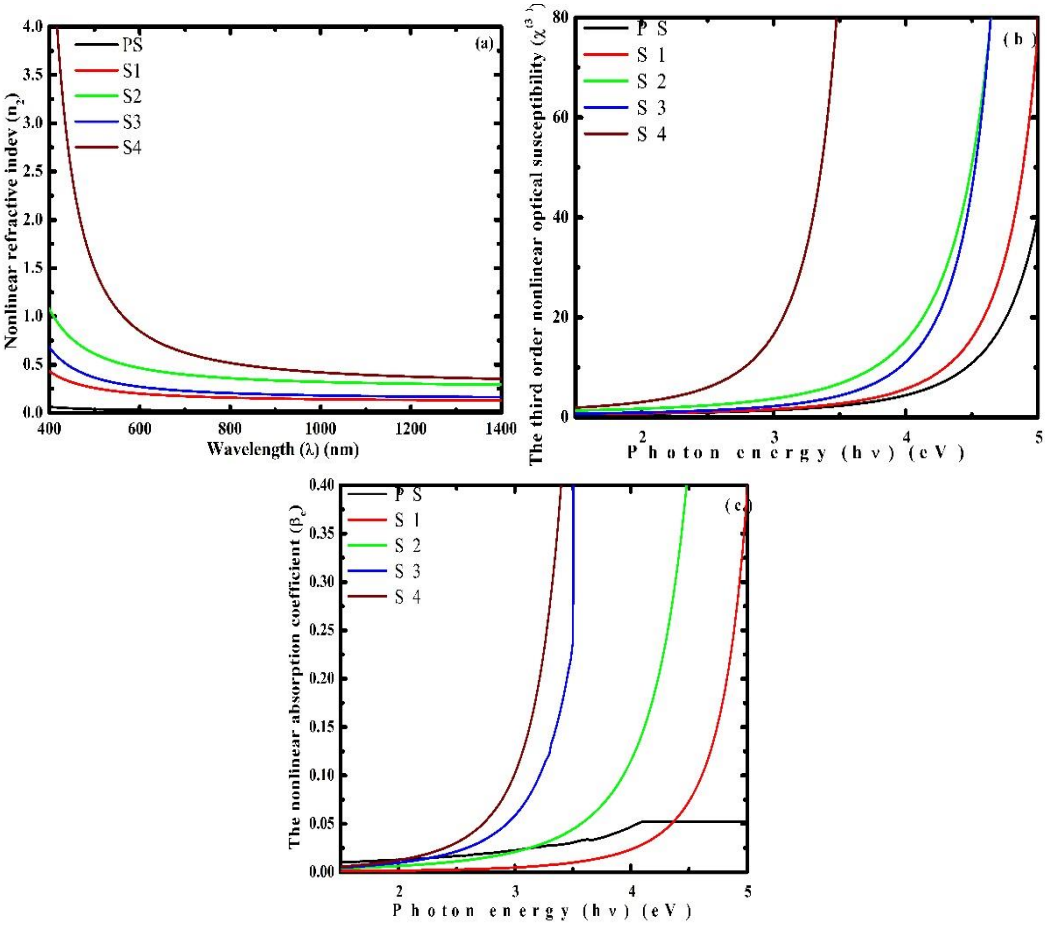

Figure 5. (**a**) Relation between n_2 and λ; (**b**) dependence of ($\chi^{(3)}$) on hν; (**c**) The influence of hν on β_c for ZnO films doped with Fe_2O_3.

3.3. Electrical results.

Electrical susceptibility $\chi_{(e)}$ means that the materials' ability for changing its electrical properties under the action of the electric field, and was determined as [52]:

$$\chi_{(e)} = \frac{\left(n^2 - k^2 - \varepsilon_o\right)}{4\pi}$$

Figure 6(a) shows the relation between $\chi_{(e)}$ and hν, $\chi_{(e)}$ increases with filler this is due to increasing the electron mobility. The relative permittivity ε_r was calculated using the following relation [53]

$$\varepsilon_r = (\chi_e + 1)$$

The relation between ε_r and hν for these films is shown in Figure 6(b). It is clear that the values of ε_r increase with filler concentrations. This could be attributed to the electron mobility increases with filler.

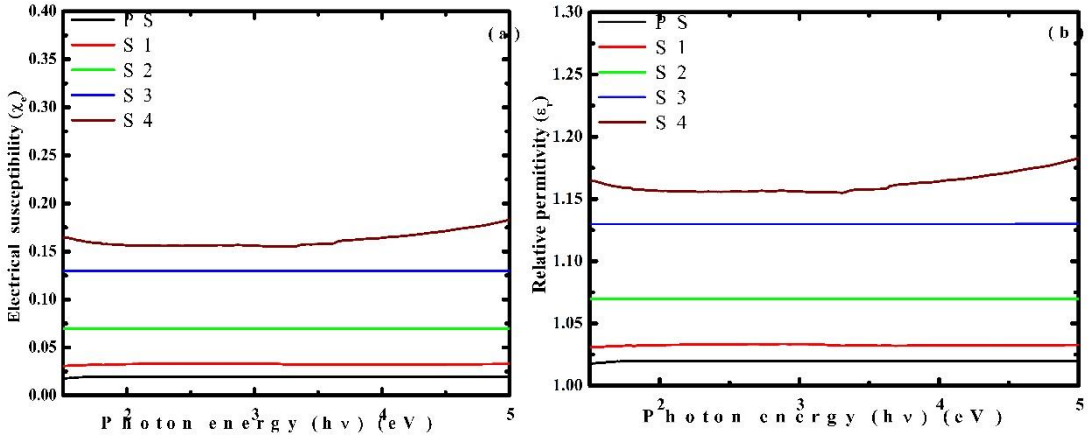

Figure 6. The influence of hν on both of (**a**) χ_e; (**b**) on ε_r for ZnO films doped with Fe_2O_3.

4. Conclusions

E_d and E_o values for ZnO/Polystyrene composite films decreased with Fe_2O_3 dopants (E_d from 8.30 to 4.90 eV), and also E_o had the values from (6.10 to 4.30 eV). The values of N/m* increased with filler, which increases free carrier. The values of M_{-1} and M_{-3} decrease with filler and also n_o decrease slightly with filler ratios. $\varepsilon^{\backslash}$ and $\varepsilon^{\backslash\backslash}$ increase with filler ratios due to increasing packing factor of these samples with filler. Both σ_1 and σ_2 increase with filler as a result of increasing electron mobility. Moreover, $\chi^{(1)}$ and the values of n_2 increase with filler ratios as a result of increasing the packing density of the investigated samples. The filler ratios affected $\chi^{(3)}$ values which increased with filler due to the increase of excited electrons. This means that these samples highly responded to change their optical properties with filler. The nonlinear absorption coefficient β_c increased with hν for these samples. Also, both $\chi_{(e)}$ and ε_r increase with increasing filler. This means that the samples' ability to change their electrical properties with electric field increases with filler concentrations increment. Finally, it is clear that the filler ratios play a very important role in enhancing most of the samples' transparent properties, especially nonlinear optical properties. Therefore, these samples could be considered a promising material for nonlinear optical applications such as optical signal processing, optical computers, ultrafast switches, ultra-short pulsed lasers, sensors, laser amplifiers.

Funding

This research received no external funding.

Acknowledgments

This research has no acknowledgment.

Conflicts of Interest

The authors declare no conflict of interest.

References

1. Selvam S.; Seerangaraj V.; LewisOscar F.; Raja S.; Kathirvel B.; Arivalagan P. Natural organic and inorganic–hydroxyapatite biopolymer composite for biomedical applications. *Progress in Organic Coatings* **2020**, *147*, 105858. https://doi.org/10.1016/j.porgcoat.2020.105858

2. Weibin Z.; Yi X.; Xiaoting W.; Tao Y.; Changren Z. Synthesis and characterization of multifunctional organic-inorganic composite hydrogel formed with tissue-adhesive property and inhibiting infection. *Materials Science and Engineering: C* **2021**, *118*, 111532. https://doi.org/10.1016/j.msec.2020.111532.
3. Kanaujia, K.; Mohammad, A.; Kshetra M.De.; Prakash G.V. Facile growth and re-crystallization of polymer-based inorganic-organic 2D hybrid composites and their applications. *Journal of Alloys and Compounds* **2020**, *829*, 154550. https://doi.org/10.1016/j.jallcom.2020.154550
4. Hilon H. Recent advances of polymeric phase change composites for flexible electronics and thermal energy storage system. *Composites Part B: Engineering* **2020**, *195*, 108094. https://doi.org/10.1016/j.compositesb.2020.108094.
5. Walker, J.P.; Asher, S.A. Acetylcholinesterase-Based Organophosphate Nerve Agent Sensing Photonic Crystal. *Analytical Chemistry* **2005**, *77*, 1596–1600. https://doi.org/10.1021/ac048562e
6. Gao, Q.,;Xu, W.; Xu, Y.; Wu, D.; Sun, Y.; Deng, F.; Shen, W. Amino Acid Adsorption on Mesoporous Materials: Influence of Types of Amino Acids, Modification of Mesoporous Materials, and Solution Conditions. *J Phys. Chem. B* **2008**, *112*, 2261–2267. https://doi.org/10.1021/jp0763580
7. Andrea, J.O.; Akiko, H.; Jenny, M. K.; Shogo, S.; Geoffrey, W. S.; Yu, K. Amino Acid Adsorption onto Mesoporous Silica Molecular Sieves. *Separation and Purification Technology* **2006**, *48*, 197–201. https://doi.org/10.1016/j.seppur.2005.07.007
8. Joanna, G.; Anna, O.; Robert, P. Comparison of ordered mesoporous materials sorption properties towards amino acids. *Adsorption* **2013**, *19*, 581–588. https://doi.org/10.1007/s10450-013-9481-z.
9. Etienne, M.; Bessiere, J.; Walcarius, A. Voltammetric Detection of Copper(II) at a Carbon Paste Elec trode Containing an Organically Modified Silica. *Sensors and Actuators B* **2001**, *76*, 531–538. https://doi.org/10.1016/S0925-4005(01)00614-1
10. Walcarius, A.; Luethi, N.; Blin, J.L.; Su, B.L.; Lamberts, L. Electrochemical Evaluation of PolysiloxaneImmobilized Amine Ligands for the Accumulation of Copper (II) Species. *Electrochemica Acta* **1999**, *44*, 4601–4610. https://doi.org/10.1016/S0013-4686(99)00181-4.
11. Jumril, Y.; Budi, M.;, Ida, H.; Muzalifah, M. S.; Roer, E. P.; Wan A. F.W.A.; Ayub, S.; Azrul A.H.; Rhonira' L.; Burhanuddin, Y.M. Polymer-Based MEMS Electromagnetic Actuator for Biomedical Application: A Review. *Polymers* **2020**, *12*, 1184. https://doi.org/10.3390/polym12051184
12. Feroz, S.; Muhammad, N.; Ratnayake, J.; G. Dias, Keratin-based materials for biomedical applications. *Bioactive Materials* **2020**, *5*, 496–509. https://doi.org/10.1016/j.bioactmat.2020.04.007
13. Oladele, I.O.; Adediran, A.A.; Akinwekomi, A.D.; Adegun, M.H.; Olumakinde, O.O.; Daramola, O.O. Development of ecofriendly snail shell particulate-reinforced recycled waste plastic composites for automobile application. *The Scientific World Journal* **2020**, *2020*, 8 pages. https://doi.org/10.1155/2020/7462758
14. Ganesan, V.; Walcarius, A. Ion Exchange and Ion Exchange Voltammetry with Functionalized Mesoporous Silica Materials. *Materials Science and Engineering B* **2008**, *149*, 123–132. https://doi.org/10.1016/j.mseb.2007.11.022
15. Liu, F.; Xiaobin, Z.; Wenchun, L.; Jipeng, C.; Xinyong, T.; Yu, L.; Lie, S. Investigation of the electrical conductivity of HDPE composites filled with bundle-like MWNTs. *Composites A* **2009**, *40*, 1717–721. https://doi.org/10.1016/j.compositesa.2009.08.004
16. Schexnailder, P.; Schmidt, G. Nano composite polymer hydrogels. *Colloid Polym Sci* **2009**, *287*, 1–11. https://doi.org/10.1007/s00396-008-1949-0
17. Nalimova, S.S.; Kondratev, V.M.; Ryabko, A.A.; Maksimov, A.I.; Moshnikov, V.A. Study of sensor properties of zinc oxide based nanostructures. *Journal of Physics: Conference Serial* **2020**, *1658*, 012033,. https://doi.org/10.1088/1742-6596/1658/1/012033.
18. Ishan, C.; Ravi, S.; Arvind, S.; Raina, K.K. Effect of excitation wavelength and europium doping on the optical properties of nanoscale zinc oxide. *Journal of Materials Science: Materials in Electronics* **2020**, *31*, 20033–20042. https://doi.org/10.1007/s10854-020-04525-x
19. Ali, A.I.; Ammar, A.H.; Abdel Moez, A. Influence of substrate temperature on structural, optical properties and dielectric results of nano- ZnO thin films prepared by Radio Frequency technique. *Superlattices and Microstructures* **2014**, *65*, 285–298. https://doi.org/10.1016/j.spmi.2013.11.007
20. Theopolina, A.; Likius, S.D.; Veikko, U.; Nelson, Y.D.; Nora, H. d-L. Structural and Optical Properties of ZnO Thin Films Prepared by Molecular Precursor and Sol–Gel Methods. *Crystals* **2020**, *10*, 132–142. https://doi.org/10.3390/cryst10020132

21. Anbuselvan, D.; Nilavazhagan,S.; Santhanam,A.; Chidhambaram, N.; Gunavathy, K.V.; Tansir A.; Saad M.A. Room temperature ferromagnetic behavior of nickel-doped zinc oxide dilute magnetic semiconductor for spintronics applications. *Physica E* **2021**, *129*, 114665. https://doi.org/10.1016/j.physe.2021.114665
22. Shamsu, A.; Naimah, K.; Siti, Fatimah A- R.; Tan, S.T.; Mohd, N. H.; Zainal, A.T.; Suresh, S.; Suriati, P. Fabrication and characterization of nanostructured zinc oxide on printed microcontact electrode for piezoelectric applications. *Journal of Materials Research and Technology* **2020**, *9*, 15952–15961. https://doi.org/10.1016/j.jmrt.2020.11.038
23. Zhang, L.; Cheng, H.; Zong, R.; Zhu, Y. Photocorrosion Suppression of ZnO Nanoparticles via Hybridization with Graphite-like Carbon and Enhanced Photocatalytic Activity. *Journal of Physical Chemistry C* **2009**, *113*, 2368– 2374. https://doi.org/10.1021/jp807778r
24. Meysam, T.; Ahmad, T.; Zohreh, M.; Byeong, K.L. Photocorrosion suppression and photoelectrochemical (PEC) enhancement of ZnO via hybridization with graphene nanosheets. *Applied Surface Science* **2020**, *502*, 144189. https://doi.org/10.1016/j.apsusc.2019.144189
25. Dindar, B.; Içli, S. Unusual photoreactivity of zinc oxide irradiated by concentrated sunlight. *Journal of Photochemistry and Photobiology A* **2001,** *140*, 263–268. https://doi.org/10.1016/S1010-6030(01)00414-2.
26. Jovana, D.; Christian, P.; Roland, S. In situ XRD study of mixed $CuInSe_2$–$CuInS_2$ formation. *Journal of Physics and Chemistry of Solids* **2004**, *64*, 1843–1848. https://doi.org/10.1016/S0022-3697(03)00248-8.
27. Ali, A.S., Ambreen, N., Bushara, F., Khan, W., Naqvi, A.H. Investigation on structural, optical and dielectric properties of Co doped ZnO nanoparticles synthesized by gel-combustion route. *Materials Science and Engineering: B* **2012**, *177*, 428–435. https://doi.org/10.1016/j.mseb.2012.01.022
28. Faisal, M.; Farid, A. H.; Mohammed J.; Mabkhoot A.; Al-Sayari, S.A.; Al- Assiri, M.S. Polythiophene doped ZnO nanostructures synthesized by modified sol-gel and oxidative polymerization for efficient photodegradation of methylene blue and gemifloxacin antibiotic. *Materials Today Communications* **2020**, *24*, 101048. https://doi.org/10.1016/j.mtcomm.2020.101048.
29. Quraish, A.K.; Riyadh, M.A.; Rawaa, A.A.; Alwan, N.J. Synthesis of Zinc Oxide / Polystyrene Nanocoposite Films and Study of Antibacterial Activity against Escherichia Coli and Staphylococcus Aures. *Nanoscience and Nanotechnology* **2016**, *6*, 1–5. https://doi.org/10.5923/j.nn.20160601.01.
30. Shankarananda; Arunkumar, L.; Sangshetty, K. Chemical Oxidation Method for Synthesis of Polyaniline–In_2O_3 Composites. *International Journal of Engineering and Science* **2012**, *1*, 59–64.
31. Kazuhiko, K.; Yuki, U.; Takashi, N. Rapid *in situ* synthesis of polymer-metal nanocomposite films in several seconds using a CO_2 laser. *Sci Rep* **2018**, *8*, 14719–14726. https://doi.org/10.1038/s41598-018-33006-9
32. Dong, W.C.; Byoung, C.K. Characterization on polystyrene/zinc oxide nanocomposites prepared from solution mixing. *Polymers for Advanced Technologies* **2005**, *16*, 846–850. https://doi.org/10.1002/pat.673
33. Nenna, G.; De Girolamo, D-M. A.; Massera, E.; Bruno, A.; Fasolino, T., Minarin, C. Optical Properties of Polystyrene-ZnO Nanocomposite Scattering Layer to Improve Light Extraction in Organic Light-Emitting Diode. *Journal of Nanomaterials* **2012**, *2012*, 319398–319404. https://doi.org/10.1155/2012/319398
34. Mulayam, S.G.; Pramod, K.Sh.; Ramvir, S.C. Optical and Thermo Electrical Properties of ZnO Nano Particle Filled Polystyrene. *Journal of Applied Polymer Science* **2010**, *118*, 2833–2840. https://doi.org/10.1002/app.32422
35. Jeeju, P.P.; Jayalekshmi, S. On the Interesting Optical Properties of Highly Transparent, Thermally Stable, Spin-Coated Polystyrene/Zinc Oxide Nanocomposite Films. *Journal of Applied Polymer Science* **2011**, *120*, 1361–1366. https://doi.org/10.1002/app.33188
36. Vijaya, S.S.; Manisha, C.G. Evolution of the optical properties of Polystyrene thin films filled with Zinc Oxide nanoparticles. *International Journal of Scientific & Engineering Research* **2013**, *4*, 2700–2705.
37. Abomostafa, H.; El komy, G.M.; Gad, S.A.; Selim, M.M. Tuning the optical properties of Fe_2O_3 doped ZnO / Polystyrene composite films. *IOSR-JAP* **2018**, *10*, 47–56.
38. Jeeju, P.P.; Jayalekshmi, S.; Chandrasekharan, K.; Sudheesh, P. Enhanced linear and nonlinear optical properties of thermally stable ZnO/poly(styrene)–poly (methyl methacrylate) nanocomposite films. *Thin Solid Films* **2013**, *531*, 378–384. https://doi.org/10.1016/j.tsf.2012.12.043
39. Jeeju, P.P.; Jayalekshmi, S.; Chandrasekharan, K.; Sudheesh, P. Size dependent nonlinear optical properties of spin coated zinc oxide-polystyrene nanocomposite films. *Optics Communications* **2012**, *285*, 5433–5439. https://doi.org/10.1016/j.optcom.2012.07.078
40. Gad, S.A.; Abdel Moez, A. Enhanced Optical Conductivity, Nonlinear Optical and Semiconducting Properties of Mg1-xCuxO/PMMA Nanocomposite. *Journal of Inorganic and Organometallic Polymers and Materials* **2020**, *30*, 469–476, https://doi.org/10.1007/s10904-019-01205-0

41. Ali, A.I; ElMeleegi, H.A.; Abdel Moez, A. Investigation of structural, optical dielectrical and optical conductivity properties of $BaTiO_3$, $Al_{0.01}$ $Ba_{0.99}$ $TiO_3$and $La_{0.01}Ba_{0.99}TiO_3$thin films prepared by pulsed laser deposition. *Phys. Scr*. **2019**, *94*, 125810-125819. Doi: 10.1088/1402-4896/ab1f25
42. Wempl, S. H.; DiDomenico, Jr. M. Optical Dispersion and the Structure of Solids. *Phys. Rev. Lett.* **1970**, *23*, 1156–1160. https://doi.org/10.1103/PhysRevLett.23.1156
43. Anshu, K.; Sharma, A. Study of Se based quaternary Se Pb (Bi,Te) chalcogenide thin films for their linear and nonlinear optical properties. *Optik* **2016**, *127*, 48–54. https://doi.org/10.1016/j.ijleo.2015.09.228
44. Aleksandra, B.D.; Herbert L. Modeling the optical properties of sapphire (α-Al_2O_3). *Optics Communications* **1998**, *157*, 72–76. https://doi.org/10.1016/S0030-4018(98)00503-3
45. Ammar, A.H.; Frid, A.M.; Sayam, M.A.M. Heat treatment effect on the structural and optical properties of $AgInSe_2$ thin films. *Vacuum* **2002**, *66*, 27–38. https://doi.org/10.1016/S0042-207X(01)00417-1
46. Fritz, S.E.; Kelley, T.W.; Frisbie, C.D. Effect of Dielectric Roughness on Performance of Pentacene TFTs and Restoration of Performance with a Polymeric Smoothing Layer. *J. Phys. Chem. B* **2005**, *109*, 10574–10577. https://doi.org/10.1021/jp044318f
47. Stolen, R.H.; Ashkin, A. Optical Kerr effect in glass waveguide. *Applied Physics Letters* **1973**, *22*, 294–297. https://doi.org/10.1063/1.1654644
48. Tichá, H.; Tichy, L. Semiempirical relation between nonlinear susceptibility (refractive index), linear refractive index and optical gap and its application to amorphous chalcogenides. *Journal of Optoelectronics and Advanced Material* **2002**, *4*, 381–386.
49. Zhou, P.; You, G.; Li, J.; Wang, S.; Qian, S.; Chen, L. Annealing effect of linear and nonlinear optical properties of Ag: Bi_2O_3 nanocomposite films. *Optics Express* **2005**, *13*, 1508–1514, https://doi.org/10.1364/OPEX.13.001508
50. Ziabari, A.A.; Ghodsi, F.E. Optoelectronic studies of sol–gel derived nanostructured CdO–ZnO composite films. *Journal of Alloys and Compounds* **2011**, *509*, 8748–8755. https://doi.org/10.1016/j.jallcom.2011.06.050
51. Beata, D.; Bouchta, S.; Xuan, N.P.; Waclaw, B. Nonlinear optical properties in ZnSe crystals. *International Conference on Solid State Crystals Proceedings of SPIE* **2001**, *4412*, 337-341.
52. Gupta, V.; Mansingh, A.I. Influence of post deposition annealing on the Structural and optical properties of sputtered zinc oxide film. *Journal of Applied Physics* **1996**, *80*, 1063. https://doi.org/10.1063/1.362842
53. Braslavsky, S.E. Glossary of terms used in photochemistry. *Pure Appl. Chem.* **2007**, *79*, 293–465. https://doi.org/10.1351/pac200779030293.